

A benchmark for dynamic rotor systems

Apostolos Doris
Mechanical Engineering Department
Dynamics and Control Group
Technical University of Eindhoven
a.doris@tue.nl

1 Model of the dynamic rotor system

¹ In this report, we present a dynamic model of an experimental dynamic rotor system. This system is depicted schematically in figure 1. By θ_u and θ_l we denote the angular displacements of the upper and lower disc, respectively. Moreover, $\omega_u = \dot{\theta}_u$ and $\omega_l = \dot{\theta}_l$ represent the angular velocities of the upper and lower disc, respectively. Furthermore, $\alpha = \theta_u - \theta_l$ represents the relative angular displacement of the lower disc with respect to the upper disc. In the sequel, we will use a state vector x defined by $x = [\alpha \quad \omega_u \quad \omega_l]^T$. The equations of motion of the system are given by:

$$\begin{aligned} J_u \ddot{\theta}_u + k_\theta(\theta_u - \theta_l) + T_{fu}(\dot{\theta}_u) &= k_m u \\ J_l \ddot{\theta}_l - k_\theta(\theta_u - \theta_l) + T_{fl}(\dot{\theta}_l) &= 0, \end{aligned} \quad (1)$$

where u is the input voltage to the power amplifier of the motor, J_u and J_l are the moments of inertia of the upper and lower discs about their respective centers of mass, k_θ is the torsional spring stiffness and k_m is the motor constant. T_{fu} and T_{fl} denote friction torques acting on the upper and lower discs. It should be noted that the friction torque at the upper disc $T_{fu}(\dot{\theta}_u)$ is due to friction in the bearings of the upper disc and due to the electro-magnetic effect in the DC-motor and the friction torque at the lower disc $T_{fl}(\dot{\theta}_l)$ comprises the friction in the bearings of the lower disc and the friction induced by a brake-mechanism (for more details see [1]).

Hereto, the following set-valued force laws for the friction in the upper and lower discs are used:

$$T_{fu}(\dot{\theta}_u) \in \begin{cases} T_{cu} \text{sign}(\dot{\theta}_u), & \dot{\theta}_u \neq 0 \\ [-T_{cu}(0^-), T_{cu}(0^+)], & \dot{\theta}_u = 0, \end{cases} \quad (2)$$

$$T_{fl}(\dot{\theta}_l) \in \begin{cases} T_{cl} \text{sign}(\dot{\theta}_l), & \dot{\theta}_l \neq 0 \\ [-T_{cl}(0^-), T_{cl}(0^+)], & \dot{\theta}_l = 0, \end{cases} \quad (3)$$

where the velocity dependency of the friction at the upper disc is expressed through $T_{cu}(\dot{\theta}_u)$, with

$$T_{cu}(\dot{\theta}_u) = T_{su} + \Delta T_{su} \text{sgn}(\dot{\theta}_u) + b_u |\dot{\theta}_u| + \Delta b_u \dot{\theta}_u, \quad (4)$$

and the velocity dependency of the friction at the lower disc is expressed through $T_{cl}(\dot{\theta}_l)$, consisting of a Stribeck model with viscous friction:

$$T_{cl}(\dot{\theta}_l) = T_{cl} + (T_{sl} - T_{cl}) e^{-|\dot{\theta}_l / \omega_{sl}|^{\delta_{sl}}} + b_l |\dot{\theta}_l|. \quad (5)$$

Equation (4) expresses the fact that we model the friction at the upper disc as a combination of static friction and viscous friction and that it is asymmetric. Herein, $T_{cu}(0^+) = T_{su} + \Delta T_{su}$ and $-T_{cu}(0^-) = -T_{su} + \Delta T_{su}$ represent the maximum and minimum value of the friction torque for zero angular velocities and $b_u + \Delta b_u$ and $b_u - \Delta b_u$ are viscous friction coefficients for positive and negative velocities, respectively. In (5), T_{cl} and T_{sl} represent the Coulomb friction and static friction levels, respectively, ω_{sl} is the Stribeck velocity, δ_{sl} the Stribeck shape parameter and b_l the viscous friction coefficient. Figure 2 shows the friction models used to describe the friction in the upper and lower disc. In Table 1 the values of the aforementioned parameters are presented.

¹part of the text of this report is taken from [1].

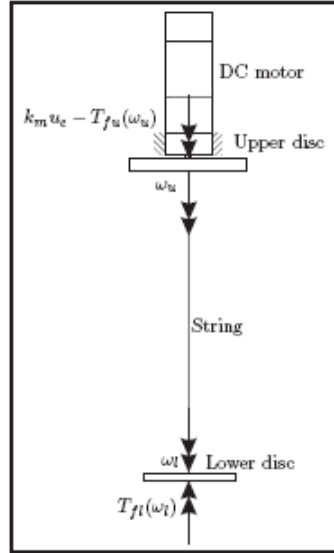


Figure 1: Schematic representation of the dynamic rotor system.

Table 1: Parameter values of the models (1), (2) and (3).

Parameter	Estimated value
J_u [kg m ² /rad]	0.4765
k_m [Nm/V]	3.9950
b_{up} [Nms/rad]	2.2247
k_θ [Nm/rad]	0.0727
J_l [kg m ² /rad]	0.0326
T_{sl} [Nm]	0.1642
T_1 [Nm]	0.0603
T_2 [Nm]	-0.2267
w_1 [s/rad]	5.7468
w_2 [s/rad]	0.2941
b_l [Nms/rad]	0.0109

2 Bifurcation Diagram

Here we analyze the steady-state behaviour (equilibria and limit cycles) of (1), with parameters as in Table 1. More specifically, a bifurcation diagram with u as a bifurcation parameter is presented. According to Figure 3 in $u = 0.2[V]$ a Hopf bifurcation occurs, which gives rise the limit cycles. Using a path following technique in combination with a shooting method [2] and [3], these limit cycles are computed numerically. Herein, the so-called switch model [4] is used to properly deal with the discontinuities in the dynamics, related to the set-valued nature of the friction models. In this figure, the maximal and minimal values of u_l are plotted when a limit cycle is found. Floquet multipliers, corresponding to these limit cycles, are computed numerically and used to determine the local stability properties of these limit cycles. Based on the presented Figure the following remarks can be made: 1) For $u < 0.2[V]$, an equilibrium set exists indicated by branch ε_1 . 2) For $u = 0.2[V]$, a subcritical Hopf bifurcation point occurs. For $u > 0.2[V]$, an unstable equilibrium branch e_3 occurs and a periodic branch p_2 that consists only of locally stable limit-cycles with stick-slip, due to the nonsmooth nonlinearities in the friction torque at the lower disc. 3) For some higher constant input voltage u (point E) the locally stable periodic branch p_2 disappears through another discontinuous fold bifurcation. At this fold bifurcation point the stable periodic branch p_2 merges with an unstable periodic branch p_3 . 4) The unstable periodic branch p_3 is connected to the equilibrium branches e_3 and e_4 in the subcritical Hopf bifurcation point C .

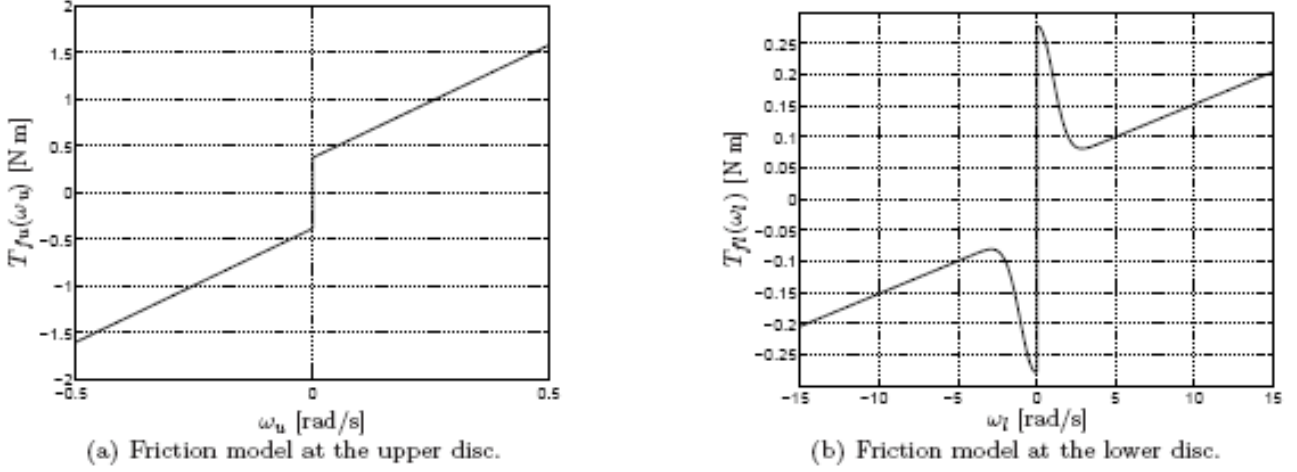


Figure 2: Friction models of the upper and lower disc of the dynamic rotor system.

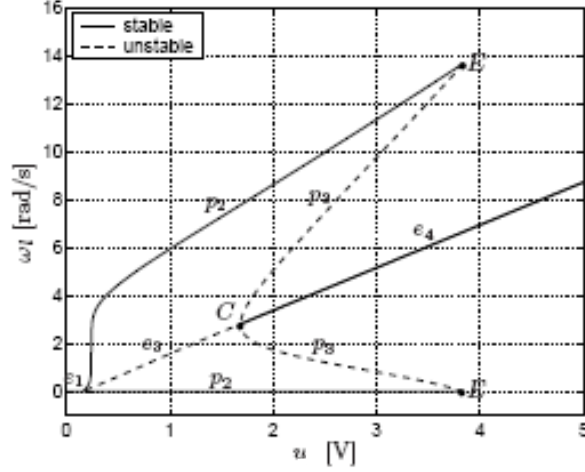


Figure 3: Bifurcation diagram of system (1) with parameters as in table 1.

3 Lagrangian form of the dynamic rotor system

An efficient way to import the friction of the upper and the lower disc of the examined system in the Siconos platform is by using the function `NewtonImpactFrictionLaw` (in the example `Dry Friction Oscillator` it is shown how this function works). In order to make use of this function in the examined system, we introduce two additional degrees-of-freedom (DOFs). We denote these DOFs as x_u and x_l . The vectors of x_u and x_l are perpendicular with respect to the vectors of the rotational velocities of the upper and lower disc, respectively. Having introduced these DOFs the Lagrangian form of the examined dynamic rotor system can be written as:

$$M(q)\ddot{q} + NNL(q, \dot{q}) + F_{Int}(q, \dot{q}) = F_{ext}(t) + r, \quad (6)$$

where

$$q = \begin{bmatrix} \theta_u \\ \theta_l \\ x_u \\ x_l \end{bmatrix}, \quad (7)$$

$$M(q) = \begin{bmatrix} J_u & 0 & 0 & 0 \\ 0 & J_l & 0 & 0 \\ 0 & 0 & 1 & 0 \\ 0 & 0 & 0 & 1 \end{bmatrix}, \quad (8)$$

$$NNL(q, \dot{q}) = C\dot{q} + K_s q, \quad (9)$$

$$C = \begin{bmatrix} b_u & 0 & 0 & 0 \\ 0 & b_l & 0 & 0 \\ 0 & 0 & 0 & 0 \\ 0 & 0 & 0 & 0 \end{bmatrix}, \quad (10)$$

$$K_s = \begin{bmatrix} k_{nl} & -k_{nl} & 0 & 0 \\ -k_{nl} & k_{nl} & 0 & 0 \\ 0 & 0 & 0 & 0 \\ 0 & 0 & 0 & 0 \end{bmatrix}, \quad (11)$$

$$F_{Int}(t) = \begin{bmatrix} \Delta T_{su} + \Delta b_u |\dot{\theta}_u| \\ 0 \\ T_{su} \\ T_{cl} + (T_{sl} - T_{cl}) e^{-|\dot{\theta}_l / \omega_{sl}|^{\delta_{sl}}} \end{bmatrix}. \quad (12)$$

$$F_{Ext}(t) = \begin{bmatrix} k_m u \\ 0 \\ 0 \\ 0 \end{bmatrix}. \quad (13)$$

The model output consists of the angular velocities $\dot{\theta}_u$ and $\dot{\theta}_l$ of the upper and lower disc, respectively:

$$y = H^T \dot{q}. \quad (14)$$

with

$$H = \begin{bmatrix} 1 & 0 & 0 & 0 \\ 0 & 1 & 0 & 0 \end{bmatrix}. \quad (15)$$

4 Comparison of numerical results of the dynamic rotor system

² In this section, we will provide numerical results of system (1) using two codes implemented on MATLAB and one implemented on the siconos platform. One of the matlab codes is based on the theory of [2], [3] and [4] (switch model) and the second one (pmodel) was developed under the frame of WP2 and WP4 by Petri Piirionen.

In Figures 4, 5, 6 and 7, we present time domain results of $\dot{\theta}_u$ and $\dot{\theta}_l$ for different inputs. More specifically, in Figure 4 we show the stable limit cycle of $\dot{\theta}_l$ and the unique response of $\dot{\theta}_u$, which is a stable equilibrium, for an input of 1.5[V]. In Figure 5 we show the stable limit cycle of $\dot{\theta}_l$ and the unique response of $\dot{\theta}_u$ for an input of 2.5[V]. In Figure 5 the stable equilibrium of $\dot{\theta}_l$ and the unique response of $\dot{\theta}_u$ are plotted for an input of 2.5[V]. Finally, in Figure 7 we show the unique responses of $\dot{\theta}_l$ and $\dot{\theta}_u$ for an input of 4.5[V].

Note that, due to the fact that the three codes give exactly the same results for the response of $\dot{\theta}_u$, ($\dot{\theta}_u$ is a stable equilibrium for all the inputs u), we will only include its plot once in every Figure.

²The work of this section was made together with Petri Piirionen, who is with University of Bristol in the group of Bristol Center of Applied Mathematics. email: Petri.Piirionen@bristol.ac.uk

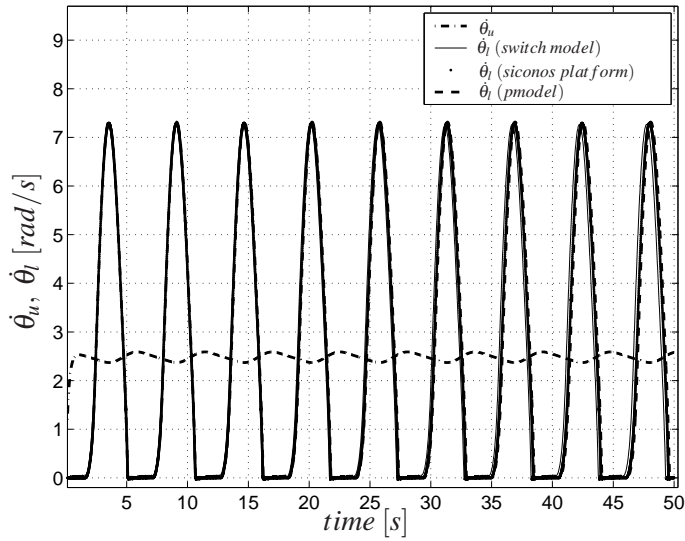


Figure 4: Upper disc lower disc velocities (equilibrium and limit cycle, respectively) for an input $u = 1.5[V]$.

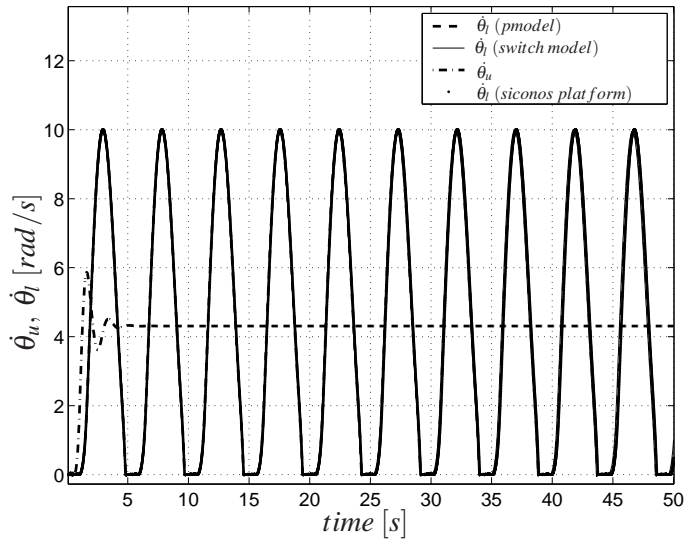


Figure 5: Upper and lower disc velocities (equilibrium and limit cycle, respectively) for an input $u = 2.5[V]$.

References

- [1] Torsional and Lateral Vibrations in Flexible Rotor Systems with Friction, PhD thesis, N. Mihajlovic, Eindhoven: Technical University of Eindhoven, 2004.
- [2] Ascher, U. M., Mattheij, R. M. M. and Russell, D. R. Numerical Solution of Boundary Value Problems for Ordinary Differential Equations. SIAM, Philadelphia, 1995.
- [3] Parker, T. S. and Chua, L. O. Practical Numerical Algorithms for Chaotic Systems. Springer- Verlag, 1989.
- [4] Leine, R. I. and Nijmeijer, H. Dynamics and Bifurcations of Non-smooth Mechanical Systems. Springer, Berlin, 2004.

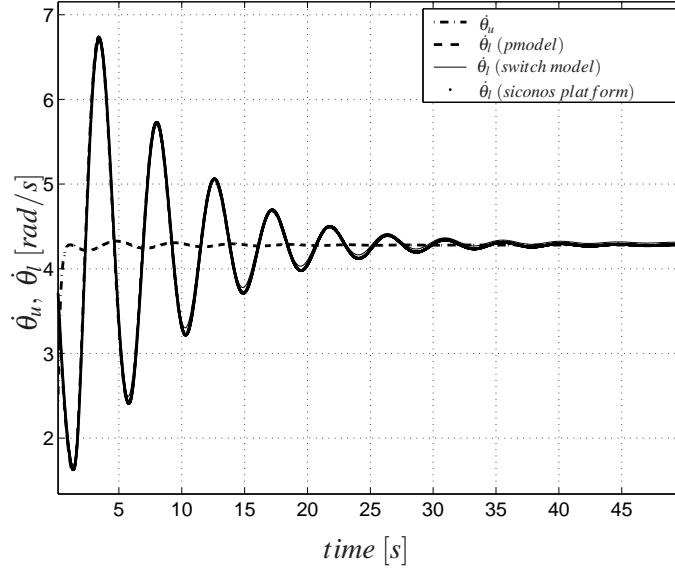


Figure 6: Upper and lower disc velocities (equilibria) for an input $u = 2.5[V]$.

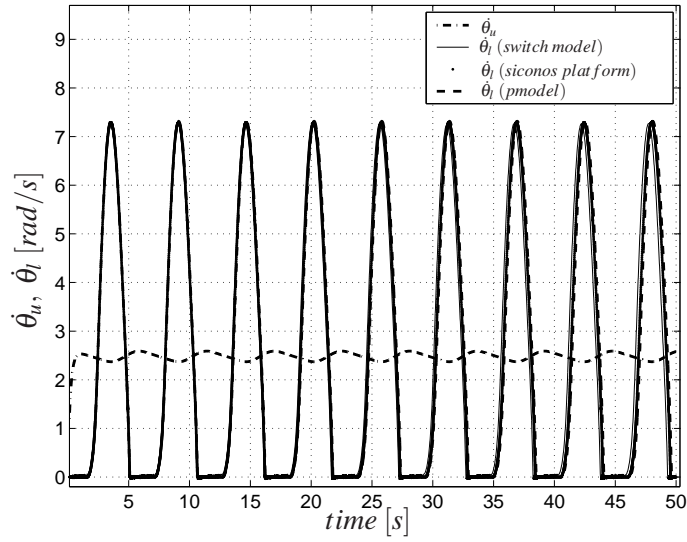


Figure 7: Upper and lower disc velocities (equilibria) for an input $u = 4.5[V]$.